

## PROPAGATION OF ELECTROMAGNETIC WAVES GUIDED BY THE ANISOTROPICALLY CONDUCTING MODEL OF A TAPE HELIX SUPPORTED BY DIELEC- TRIC RODS

Natarajan Kalyanasundaram<sup>1</sup> and Gnanamoorthi N. Babu<sup>2</sup>

<sup>1</sup>Jaypee Institute of Information Technology, A-10, Sector 62,  
Noida 201307, India

<sup>2</sup>Shiv Nadar University, Village Chithera, Greater Noida 203207, India

**Abstract**—The practically important case of a dielectric-loaded tape helix enclosed in a coaxial perfectly conducting cylindrical shell is analysed in this paper. The dielectric-loaded tape helix for guided electromagnetic wave propagation considered here has infinitesimal tape thickness and infinite tape-material conductivity. The homogeneous boundary value problem is solved taking into account the exact boundary conditions similar to the case of anisotropically conducting open tape helix model [1, 2]. The boundary value problem is solved to yield the dispersion equation which takes the form of the solvability condition for an infinite system of linear homogeneous algebraic equations viz., the determinant of the infinite-order coefficient matrix is zero. For the numerical computation of the approximate dispersion characteristic, all the entries of the symmetrically truncated version of the coefficient matrix are estimated by summing an adequate number of the rapidly converging series for them. The tape-current distribution is estimated from the null-space vector of the truncated coefficient matrix corresponding to a specified root of the dispersion equation.

### 1. INTRODUCTION

A method of exactly solving the boundary value problem arising in the propagation of slow electromagnetic waves guided by an open tape helix for the anisotropically conducting model [1], wherein the component of the tape-current density perpendicular to the winding

---

*Received 18 March 2013, Accepted 11 April 2013, Scheduled 18 April 2013*

\* Corresponding author: Natarajan Kalyanasundaram (n.kalyanasundaram@jiit.ac.in).

direction is neglected, was presented for the first time in [1, 2] without making any a priori assumption about the tape-current distribution. This method has subsequently been extended to solving the problem of guided electromagnetic wave propagation through an open tape helix for the perfectly conducting model in [3]. Beginning with the fundamental work of Sensiper [4] until the publication of [1], all the published derivations [5–8] of the propagation characteristics of electromagnetic waves guided by an open helical slow-wave structure, modeled invariably to be an anisotropically conducting tape helix, were based on some ad hoc assumption about the tape-current distribution. As a consequence, the tangential electric field boundary conditions could only be satisfied in some approximate sense. The need for such an ad hoc assumption about the tape-current distribution arose out of the inherent inability of the form of the series-expansion for the tape-current density assumed in every one of these “derivations” to correctly confine the surface current to the tape surface only. In other words, the infinite series for the tape-current density ought to have summed automatically to zero in the gap region (the region on the cylindrical surface between the tapes) but does not.

In this paper, the method analyzing the anisotropically conducting model of the open tape helix is applied to the practically relevant case of a tape helix supported inside a coaxial perfectly conducting cylindrical shell by symmetrically disposed wedge-shaped (see Fig. 1) dielectric rods. With a view to making the problem of guided electromagnetic wave propagation through such a model of slow-wave structure tractable, the azimuthally periodic dielectric constant of the tubular region between the tape helix and the outer conductor is replaced by its azimuthally-averaged constant value  $\epsilon_{eff}$ . When the cross-sectional shape of the symmetrically located dielectric support rods is anything other than a wedge  $\{(r, \theta) : a \leq r \leq b, \theta_1 \leq \theta \leq \theta_2\}$ , the azimuthally-averaged dielectric constant  $\epsilon_{eff}(r)$  will turn out to be a function of the radial coordinate  $r$ . In this case, the region between the tape helix and the outer conductor is partitioned into a finite number of tubular layers and each layer is characterized by the radially-averaged value of  $\epsilon_{eff}(r)$  over its radial thickness. This is equivalent to approximating  $\epsilon_{eff}(r)$  by a piecewise constant function in the radial variable  $r$ . The solution for the field components over the entire region between the tape helix and the outer conductor can then be obtained by enforcing the continuity of the tangential field components across the interfaces separating two adjacent tubular layers with different values for the effective dielectric constant. This procedure has been adopted by Jain et al. [9] to analyze guided wave propagation through a tape helix supported by dielectric rods of circular cross-section based of

course on an ad hoc assumption about the tape-current distribution.

Almost all of the existing literature on the propagation of electromagnetic waves guided by a dielectric-loaded tape helix are based either on an ad hoc assumption about the tape-current distribution [9–15] or an a priori assumption about the behavior of the tape-current distribution near the tape edges [17]. Tien [10] and McMurtry [11] have analysed the effects of a supporting dielectric layer surrounded by a metal tube based on a tape-current distribution used by Sensiper [4] and Watkins [6]. The same observation may be made about the work of Uhm [12] on guided electromagnetic wave propagation using the anisotropically conducting model of a dielectric-loaded tape helix. D'Agostino et al. [13] and Tsutaki et al. [14] based their analysis of guided electromagnetic wave propagation through a dielectric-loaded tape helix on an assumed cosh function dependence for the tape-current distribution whereas Kosmahl and Branch, Jr. [15] made use of a cosh function dependence for the gap fields in their analysis of guided-wave propagation supported by a dielectric-loaded tape helix. A completely different formulation in terms of helical coordinates was proposed by Chen et al. [16] to tackle the problem of guided electromagnetic wave propagation through a tape helix supported by a finite number of symmetrically located wedge-shaped dielectric rods without resorting to homogenization of the nonhomogeneous dielectric region between the tape helix and the outer conductor by azimuthal averaging. However, it was not possible to satisfy the electromagnetic boundary conditions in the gap regions of the tape helix within the framework proposed by Chen et al.

Although the derivation of the dispersion equation presented by Chernin et al. [17] for a perfectly conducting dielectric loaded tape helix involves neither any ad hoc assumption about the tape-current distribution except for its behavior near the tape edges nor any approximations in satisfying the tangential electric field boundary conditions on the tape surface, their surface-current density expansions, which are assumed to have a form identical to those of the field components when restricted to the surface of the infinite cylinder containing the tape helix, do not again seem to be capable of limiting the support of the surface-current density to the tape surface only. Moreover, reexpansions of the tape current density components in terms of Chebyshev polynomials, resorted to by Chernin et al. [17], seem to be motivated by the anticipated singularity of the surface current density component parallel to the winding direction near the tape edges. Such an a priori assumption regarding the edge behavior of the surface current density component is totally unnecessary as an ordinary Fourier-series expansion is pretty well capable of bringing

out any such singular behavior, if present, as long as the singularity is integrable. Another anomalous behavior displayed by the surface current density plots obtained by Chenin et al. concerns the lack of symmetry about the center line of the tape.

In the sequel, we make use of the following standard notations: (i)  $\mathbb{Z}$  for the ring of integers, (ii) a prime superscript on a function for the derivative with respect to the argument and (iii)  $1_X$  for the indicator function of a set  $X$ , that is

$$1_X(x) = \begin{cases} 1 & \text{if } x \in X \\ 0 & \text{if } x \notin X \end{cases}$$

## 2. PROBLEM FORMULATION

We consider a tape helix of infinite length, constant pitch and tape width, infinitesimal tape thickness and infinite tape-material conductivity surrounded by a dielectric of effective permittivity  $\epsilon_{eff}$ , enclosed in a coaxial metallic outer conductor. The axis of the helix is taken along the  $z$ -coordinate of a cylindrical coordinate system  $(\rho, \varphi, z)$ . The radius of the helix is  $a$ , the inner radius of the outer cylindrical conductor is  $b$ , the pitch is  $p$ , the width of the helix in the axial direction is  $w$ , and the pitch angle  $\psi$  is then given by  $\cot \psi = 2\pi a/p$ .

The scalar Helmholtz equation for the Borgnis potential  $U$  (and

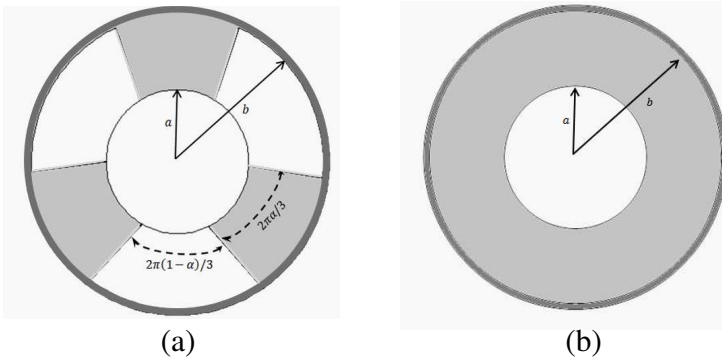


**Figure 1.** Cross sectional view of dielectric-loaded tape helix model: (a) Actual structure with three support rods of dielectric constant  $\epsilon_r$ ; (b) Azimuthally averaged structure with an effective dielectric constant  $\epsilon_{eff} = (1 - \alpha) + \alpha\epsilon_r$  for the region between the tape helix and the outer conductor.

$V$ ) is

$$\frac{1}{\rho} \frac{\partial}{\partial \rho} \left( \rho \frac{\partial U}{\partial \rho} \right) + \frac{1}{\rho^2} \frac{\partial^2 U}{\partial \varphi^2} + \frac{\partial^2 U}{\partial z^2} + k_0^2 U = 0 \tag{1}$$

Assuming solutions for  $U$  and  $V$  in the form

$$[U \quad V]^T = \sum_{n \in \mathbb{Z}} [F_n(\rho) \quad G_n(\rho)]^T e^{j(n\varphi - \beta_n z)}$$

dictated by the geometric invariance properties of the tape helix, and substituting into (1) (and the corresponding equation for  $V$ ),  $F_n$  (and  $G_n$ ) is seen to satisfy the ordinary differential equation

$$\frac{\partial^2 F_n}{\partial \rho^2} + \frac{1}{\rho} \frac{\partial F_n}{\partial \rho} - \left[ \frac{n^2}{\rho^2} + \tau_n^2 \right] F_n = 0 \quad \text{for } 0 \leq \rho < a \tag{2a}$$

$$\frac{\partial^2 F_n}{\partial \rho^2} + \frac{1}{\rho} \frac{\partial F_n}{\partial \rho} - \left[ \frac{n^2}{\rho^2} + \tau_n^{+2} \right] F_n = 0 \quad \text{for } a < \rho < b \tag{2b}$$

where  $\beta_n = \beta_0 + 2\pi n/p$  is the propagation phase constant of the  $n$ th space harmonic; the transverse mode number  $\tau_n$ ,  $n \in \mathbb{Z}$ , for the region inside helix ( $0 \leq \rho < a$ ) is given by  $\tau_n^2 \triangleq \beta_n^2 - k_0^2$ ; the transverse mode number  $\tau_n^+$ ,  $n \in \mathbb{Z}$ , for the dielectric region ( $a < \rho < b$ ) is given by  $\tau_n^{+2} \triangleq \beta_n^2 - \epsilon_{\text{eff}} k_0^2$ , where  $k_0 = \omega/c$  is the free-space wave number at the radian frequency  $\omega$ ,  $\beta_0 = \beta(\omega)$  the propagation phase constant of guided electromagnetic waves supported by the dielectric-loaded tape helix at the radian frequency  $\omega$ , and  $c = (\mu_0 \epsilon_0)^{-1/2}$  the speed of light in vacuum. Thus the Borgnis' potential for the guided-wave solutions, at the radian frequency  $\omega$ , takes on the form

$$\begin{aligned} & \begin{bmatrix} U \\ V \end{bmatrix} \\ &= \begin{cases} \sum_{n \in \mathbb{Z}} \begin{bmatrix} A_n \\ B_n \end{bmatrix} S_n(p_n \rho) e^{j(n\varphi - \beta_n z)} & \text{for } 0 \leq \rho < a \\ \sum_{n \in \mathbb{Z}} \left\{ \begin{bmatrix} C_n \\ D_n \end{bmatrix} S_n(p_n^+ \rho) + \begin{bmatrix} C'_n \\ D'_n \end{bmatrix} T_n(p_n^+ \rho) \right\} e^{j(n\varphi - \beta_n z)} & \text{for } a < \rho < b \end{cases} \tag{3} \end{aligned}$$

where  $p_n \triangleq |\tau_n|$  and  $p_n^+ \triangleq |\tau_n^+|$  and  $A_n, B_n, C_n, D_n, C'_n$  and  $D'_n$ ,  $n \in \mathbb{Z}$ , are arbitrary (complex) constants. The functions  $S_n$  and  $T_n$  appearing in (3) are given by

$$S_n(p_n \rho) = \begin{cases} I_n(p_n \rho), & \tau_n^2 > 0 \\ J_n(p_n \rho), & \tau_n^2 < 0 \end{cases}$$

$$S_n(p_n^+\rho) = \begin{cases} I_n(p_n^+\rho), & \tau_n^{+2} > 0 \\ J_n(p_n^+\rho), & \tau_n^{+2} < 0 \end{cases}$$

$$T_n(p_n^+\rho) = \begin{cases} K_n(p_n^+\rho), & \tau_n^{+2} > 0 \\ -\frac{\pi}{2}Y_n(p_n^+\rho), & \tau_n^{+2} < 0 \end{cases}$$

where  $J_n$  and  $Y_n$  are the  $n$ th order Bessel functions of first and second kind respectively, and  $I_n$  and  $K_n$  are the  $n$ th order modified Bessel functions of the first and second kind respectively. The expressions for the tangential field components may be obtained from the Borgnis potentials [7]:

$$E_z = \begin{cases} \sum_{n \in \mathbb{Z}} -p_n^2 A_n S_n(p_n \rho) e^{j(n\varphi - \beta_n z)} \\ \quad \text{for } 0 \leq \rho < a \\ \sum_{n \in \mathbb{Z}} -p_n^{+2} C_n [S_n(p_n^+ \rho) - \gamma_{bn} T_n(p_n^+ \rho)] e^{j(n\varphi - \beta_n z)}, \\ \quad \text{for } a < \rho < b \end{cases} \quad (4a)$$

$$E_\varphi = \begin{cases} \sum_{n \in \mathbb{Z}} \left[ \frac{n\beta_n}{\rho} A_n S_n(p_n \rho) + j\omega\mu_0 p_n B_n S'_n(p_n \rho) \right] e^{j(n\varphi - \beta_n z)} \\ \quad \text{for } 0 \leq \rho < a \\ \sum_{n \in \mathbb{Z}} \left[ \frac{n\beta_n}{\rho} C_n [S_n(p_n^+ \rho) - \gamma_{bn} T_n(p_n^+ \rho)] \right. \\ \quad \left. + j\omega\mu_0 p_n^+ D_n [S'_n(p_n^+ \rho) - \gamma'_{bn} T'_n(p_n^+ \rho)] \right] e^{j(n\varphi - \beta_n z)} \\ \quad \text{for } a < \rho < b \end{cases} \quad (4b)$$

$$H_z = \begin{cases} \sum_{n \in \mathbb{Z}} -p_n^2 B_n S_n(p_n \rho) e^{j(n\varphi - \beta_n z)} \\ \quad \text{for } 0 \leq \rho < a \\ \sum_{n \in \mathbb{Z}} -(p_n^+)^2 D_n [S_n(p_n^+ \rho) - \gamma'_{bn} T_n(p_n^+ \rho)] e^{j(n\varphi - \beta_n z)} \\ \quad \text{for } a < \rho < b \end{cases} \quad (5a)$$

$$H_\varphi = \begin{cases} \sum_{n \in \mathbb{Z}} \left[ -j\omega\epsilon_0 p_n A_n S'_n(p_n \rho) + \frac{n\beta_n}{\rho} B_n S_n(p_n \rho) \right] e^{j(n\varphi - \beta_n z)} \\ \quad \text{for } 0 \leq \rho < a \\ \sum_{n \in \mathbb{Z}} \left[ \left( \frac{n\beta_n}{\rho} D_n [S_n(p_n^+ \rho) - \gamma'_{bn} T_n(p_n^+ \rho)] \right) \right. \\ \quad \left. - (j\omega\epsilon_o \epsilon_{\text{eff}} p_n^+ C_n [S'_n(\tau_n^+ \rho) - \gamma_{bn} T'_n(p_n^+ \rho)]) \right] e^{j(n\varphi - \beta_n z)} \\ \quad \text{for } a < \rho < b \end{cases} \quad (5b)$$

where  $\gamma_{bn} \triangleq \frac{S_n(p_n^+ b)}{T_n(p_n^+ b)}$  and  $\gamma'_{bn} \triangleq \frac{S'_n(p_n^+ b)}{T'_n(p_n^+ b)}$ . In (4) and (5), the arbitrary

constants  $C'_n$  and  $D'_n$ ,  $n \in \mathbb{Z}$ , have been evaluated in terms of  $C_n$  and  $D_n$  respectively to be  $C'_n = -C_n \gamma_{bn}$  and  $D'_n = -D_n \gamma'_{bn}$  by enforcing the boundary conditions  $E_z = 0$  and  $E_\varphi = 0$  at  $\rho = b$ . The boundary conditions  $E_z = 0$  and  $E_\varphi = 0$  at  $\rho = b$  are equivalent to having  $U = 0$  and  $\frac{\partial V}{\partial \rho} = 0$  at  $\rho = b$ .

### 3. TAPE HELIX BOUNDARY CONDITIONS

The boundary conditions at  $\rho = a$  for the anisotropically conducting model of the dielectric loaded tape helix are

- (i) The tangential electric field is continuous for all values of  $\varphi$  and  $z$ .
- (ii) The discontinuity in the tangential magnetic field equals the surface current density on the tape surface.
- (iii) The tangential electric field vanishes on the tape surface.

Thus

$$E_z(a-, \varphi, z) - E_z(a+, \varphi, z) = 0 \tag{6a}$$

$$E_\varphi(a-, \varphi, z) - E_\varphi(a+, \varphi, z) = 0 \tag{6b}$$

$$[H_z(a-, \varphi, z) - H_z(a+, \varphi, z)] \sin \psi + [H_\varphi(a-, \varphi, z) - H_\varphi(a+, \varphi, z)] \cos \psi = 0 \tag{6c}$$

$$[H_z(a-, \varphi, z) - H_z(a+, \varphi, z)] \cos \psi - [H_\varphi(a-, \varphi, z) - H_\varphi(a+, \varphi, z)] \sin \psi = J_{||}(\varphi, z) \tag{6d}$$

$$[E_z(a, \varphi, z) + E_\varphi(a, \varphi, z) \cot \psi] g(\varphi, z) = 0 \tag{6e}$$

where  $J_{||}(\varphi, z)$  is the surface current density component parallel to the winding direction supported by helix, and the function  $g(\varphi, z)$  is defined in terms of the indicator functions  $1_{I_l(\varphi)}$ ,  $l \in \mathbb{Z}$ , of the disjoint (for the same value of  $\varphi$ ) intervals  $[(l + \varphi/2\pi)p - w/2, (l + \varphi/2\pi)p + w/2]$ ,  $l \in \mathbb{Z}$ , by

$$g(\varphi, z) \triangleq \sum_{l \in \mathbb{Z}} 1_{I_l(\varphi)}(z) \tag{7}$$

and for an arbitrary function  $f(\rho, \varphi, z)$

$$f(a\pm, \varphi, z) \triangleq \lim_{\delta \downarrow 0} f(a \pm \delta, \varphi, z)$$

The functional dependence of the surface current density component  $J_{||}(\varphi, z)$ , which is confined only to the two-dimensional region on the infinite cylinder  $\rho = a$  occupied by the tape-helix material, on the variables  $\varphi$  and  $z$  is dictated by the periodicity and the symmetry

conditions imposed by the helix geometry. Accordingly,  $J_{||}(\varphi, z)$ , admits the representation

$$J_{||}(\rho, \varphi, z) = \left( \sum_{n \in \mathbb{Z}} J_n e^{j(n\varphi - \beta_n z)} \right) g(\varphi, z) \quad (8)$$

The factor  $g(\varphi, z)$  on the right hand side of (8) ensures that the surface current is confined to the tape surface only. The surface current density expansion of (8) may be recast into the form

$$J_{||}(\varphi, z) = e^{-j\beta_0 z} f(\hat{\zeta}) \quad (9)$$

where

$$f(\hat{\zeta}) = \sum_{l \in \mathbb{Z}} \left( \sum_{n \in \mathbb{Z}} J_n e^{-j2\pi n \hat{\zeta}} \right) 1_{[l - \hat{w}/2, l + \hat{w}/2]}(\hat{\zeta}) \quad (10)$$

$$\hat{\zeta} \triangleq (z - \varphi p / 2\pi) / p \quad (11)$$

and

$$\hat{w} \triangleq w / p$$

The function  $f$ , being periodic in  $\hat{\zeta}$  with period 1, may be expanded in a Fourier series

$$f(\hat{\zeta}) = \sum_{k \in \mathbb{Z}} \Gamma_k e^{-j2\pi k \hat{\zeta}} \quad (12)$$

where the Fourier coefficients  $\Gamma_k$ ,  $k \in \mathbb{Z}$ , are given by

$$\Gamma_k = \int_{-1/2}^{1/2} f(\hat{\zeta}) e^{j2\pi k \hat{\zeta}} d\hat{\zeta} = \hat{w} \sum_{n \in \mathbb{Z}} J_n \text{sinc}(k - n) \hat{w} \quad (13)$$

where

$$\text{sinc} X \triangleq \begin{cases} \sin \pi X / \pi X & \text{if } X \neq 0 \\ 1 & \text{if } X = 0 \end{cases}$$

Thus

$$J_{||}(\varphi, z) = \sum_{n \in \mathbb{Z}} \Gamma_n e^{j(n\varphi - \beta_n z)} \quad (14)$$

Now, we are ready to tackle the boundary conditions. For the sake of convenience, let us introduce the abbreviations:

$$\begin{aligned} k_{0a} &\triangleq ak_0 \\ \beta_{na} &\triangleq a\beta_n \\ p_{na} &\triangleq ap_n, & p_{na}^+ &\triangleq ap_n^+, \\ p_{nb}^+ &\triangleq bp_n^+ = (b/a)p_{na}^+, & n &\in \mathbb{Z} \end{aligned}$$

Substituting the field expansions into the homogeneous boundary conditions (6a)–(6c) and equating the coefficients of  $\exp j(n\varphi - \beta_n z)$  for each  $n \in \mathbb{Z}$  separately to zero, we obtain the following three relations among the four arbitrary constants  $A_n, B_n, C_n$  and  $D_n$  for each  $n \in \mathbb{Z}$ :

$$C_n = \left\{ \left( \frac{p_{na}}{p_{na}^+} \right)^2 \frac{S_n(p_{na})}{\Delta_{ab}} T_n(p_{nb}^+) \right\} A_n, \quad n \in \mathbb{Z} \quad (15a)$$

$$D_n = \frac{T'_n(p_{na}^+)}{j\omega\mu_0} \frac{1}{p_{na}^+ \Delta_{\bar{a}\bar{b}}} \left\{ \begin{aligned} &n\beta_{na} S_n(p_{na}) \left( 1 - \frac{p_{na}^2}{p_{na}^{+2}} \right) A_n \\ &+ j\omega\mu_0 p_{na} S'_n(p_{na}) B_n \end{aligned} \right\} \quad (15b)$$

$$B_n = j\omega\epsilon_0 \left\{ \frac{\begin{aligned} &\frac{\Delta_{\bar{a}\bar{b}}}{\Delta_{\bar{a}\bar{b}}} \frac{1}{k_{0a}^2} \frac{S_n(p_{na})}{p_{na}^+ S'_n(p_{na})} (n\beta_{na}) \\ &\left( 1 - \frac{p_{na}^2}{p_{na}^{+2}} \right) (p_{na}^{+2} - n\beta_{na} \cot \psi) - \chi_{B_n} \end{aligned}}{\begin{aligned} &\frac{\Delta_{\bar{a}\bar{b}} p_{na}}{\Delta_{\bar{a}\bar{b}} p_{na}^+} [p_{na}^{+2} - n\beta_{na} \cot \psi] \\ &+ \frac{S_n(p_{na})}{S'_n(p_{na})} [n\beta_{na} \cot \psi - p_{na}^2] \end{aligned}} \right\} A_n \quad (15c)$$

where

$$\chi_{B_n} = p_{na} \left( \epsilon_{eff} \frac{p_{na}}{p_{na}^+} \frac{\Delta_{\bar{a}\bar{b}} S_n(p_{na})}{\Delta_{ab} S'_n(p_{na})} - 1 \right) \cot \psi$$

Substituting for  $B_n$  in terms of  $A_n$  from (15c) into (15b) gives an explicit linear relation between  $D_n$  and  $A_n$  too. The fourth boundary condition (5d) together with the explicit expressions for  $B_n, C_n$  and  $D_n$  in terms of  $A_n$  and the expression (14) for  $J_{||}(\varphi z)$ , in turn, relates  $A_n$  to  $\Gamma_n$  as

$$A_n = \frac{\Gamma_n}{j\omega\epsilon_0} \frac{1}{(1 + \cot^2 \psi) \sin \psi} \frac{1}{S'_n(p_{na})} \left\{ \begin{aligned} &\frac{S_n(p_{na})}{S'_n(p_{na})} (n\beta_{na} \cot \psi - p_{na}^2) + \frac{\Delta_{\bar{a}\bar{b}} p_{na}}{\Delta_{\bar{a}\bar{b}} p_{na}^+} (p_{na}^{+2} - n\beta_{na} \cot \psi) \\ &p_{na}^3 \left( 1 - \epsilon_{eff} \frac{p_{na}}{p_{na}^+} \frac{S_n(p_{na})}{S'_n(p_{na})} \frac{\Delta_{\bar{a}\bar{b}}}{\Delta_{ab}} \right) \left( \frac{\Delta_{\bar{a}\bar{b}} p_{na}^+}{\Delta_{\bar{a}\bar{b}} p_{na}} - \frac{S_n(p_{na})}{S'_n(p_{na})} \right) - \chi_{A_n} \end{aligned} \right\}$$

on equating the coefficients of  $\exp j(n\varphi - \beta_n z)$  on both sides of (6d) where

$$\chi_{A_n} = (n\beta_{na})^2 \frac{1}{k_{0a}^2} \frac{\Delta_{\bar{a}\bar{b}}}{\Delta_{\bar{a}\bar{b}}} \frac{S_n^2(p_{na})}{S_n'(p_{na})} \frac{p_{na}^+}{p_{na}} \left( 1 - \frac{p_{na}^2}{p_{na}^{+2}} \right) \quad (15d)$$

In (15)

$$\begin{aligned}\Delta_{ab} &= S_n(p_{na}^+) T_n(p_{nb}^+) - S_n(p_{nb}^+) T_n(p_{na}^+) \\ \Delta_{a\bar{b}} &= S_n(p_{na}^+) T'_n(p_{nb}^+) - S'_n(p_{nb}^+) T_n(p_{na}^+) \\ \Delta_{\bar{a}b} &= S'_n(p_{na}^+) T_n(p_{nb}^+) - S_n(p_{nb}^+) T'_n(p_{na}^+) \\ \Delta_{\bar{a}\bar{b}} &= S'_n(p_{na}^+) T'_n(p_{nb}^+) - S'_n(p_{nb}^+) T'_n(p_{na}^+)\end{aligned}$$

Finally, the enforcement of the homogeneous boundary condition on the tangential electric field component parallel to the winding direction leads to the functional relation

$$e^{-j\beta_0 z} \sum_{l \in \mathbb{Z}} \left( \sum_{n \in \mathbb{Z}} \sigma_n \Gamma_n e^{-j2\pi n \hat{\zeta}} \right) 1_{[l-\hat{w}/2, l+\hat{w}/2]}(\hat{\zeta}) = 0 \quad (16)$$

where

$$\sigma_n = \left\{ \begin{array}{l} p_{na}^+ (n\beta_{na} \cot \psi - p_{na}^2)^2 \\ - \chi_{\sigma_n} - k_{oa}^2 p_{na}^2 \left( \frac{S'_n(p_{na})}{S_n(p_{na})} \right)^2 \left[ \epsilon_{eff} p_{na} \frac{S_n(p_{na})}{S'_n(p_{na})} - p_{na}^+ \right] \\ \frac{p_{na}^+ 2 \cdot 2 \left( \frac{S'_n(p_{na})}{S_n(p_{na})} - \epsilon_{eff} \frac{p_{na}}{p_{na}^+} \frac{\Delta_{\bar{a}\bar{b}}}{\Delta_{ab}} \right) \left( \frac{\Delta_{\bar{a}\bar{b}} S'_n(p_{na})}{\Delta_{\bar{a}\bar{b}} S_n(p_{na})} - \frac{p_{na}}{p_{na}^+} \right)}{p_{na}^+ 2 \cdot 2 \left( \frac{S'_n(p_{na})}{S_n(p_{na})} - \epsilon_{eff} \frac{p_{na}}{p_{na}^+} \frac{\Delta_{\bar{a}\bar{b}}}{\Delta_{ab}} \right) \left( \frac{\Delta_{\bar{a}\bar{b}} S'_n(p_{na})}{\Delta_{\bar{a}\bar{b}} S_n(p_{na})} - \frac{p_{na}}{p_{na}^+} \right)} \\ - \frac{\Delta_{\bar{a}\bar{b}}}{\Delta_{\bar{a}\bar{b}}} (n\beta_{na})^2 \Delta \epsilon_{eff} \end{array} \right\} \quad (17)$$

where

$$\chi_{\sigma_n} = \frac{\Delta_{\bar{a}\bar{b}}}{\Delta_{\bar{a}\bar{b}}} p_{na} \frac{S'_n(p_{na})}{S_n(p_{na})} (n\beta_{na} \cot \psi - p_{na}^2) [n\beta_{na} \cot \psi (1 + k_{oa}^2 \Delta \epsilon_{eff}) - p_{na}^2]$$

where  $\Delta \epsilon_{eff} \triangleq \epsilon_{eff} - 1$ . Since  $e^{-j\beta_0 z} \neq 0$ , (16) implies that each Fourier coefficient of the periodic function

$$h(\hat{\zeta}) \triangleq \sum_{l \in \mathbb{Z}} \left( \sum_{n \in \mathbb{Z}} \sigma_n \Gamma_n e^{-j2\pi n \hat{\zeta}} \right) 1_{[l-\hat{w}/2, l+\hat{w}/2]}(\hat{\zeta}) \quad (18)$$

of  $\hat{\zeta}$  (with period 1) must vanish, that is

$$\sum_{n \in \mathbb{Z}} \sigma_n \Gamma_n \text{sinc}(n - k) \hat{w} = 0 \quad \text{for } k \in \mathbb{Z} \quad (19)$$

Substituting for  $\Gamma_n$  from (13), the condition (19) may be put in the form

$$\sum_{q \in \mathbb{Z}} \alpha_{kq} J_q = 0 \quad \text{for } k \in \mathbb{Z} \quad (20)$$

where

$$\alpha_{kq} = \sum_{n \in \mathbb{Z}} \sigma_n \text{sinc}(k - n)\hat{w} \text{sinc}(q - n)\hat{w} \quad (21)$$

For a nontrivial solution of the infinite set of linear homogenous Equations (20) for  $J_q$ ,  $q \in \mathbb{Z}$ , it is necessary that the determinant of the coefficient matrix  $\mathbf{A} \triangleq [\alpha_{kq}]$ ,  $k, q \in \mathbb{Z}$ , is zero, that is

$$|\mathbf{A}| = 0 \quad (22)$$

The determinantal Equation (22) gives, in principle, the dispersion relation for the cold wave modes of the dielectric supported anisotropically conducting tape helix. Similar to the analysis of anisotropically conducting open tape helix model presented in [1], the derivation of the dispersion equation is based neither on any a priori assumption regarding the tape-current distribution nor on any approximation of the helix boundary conditions. In this sense, the derivation is exactly within the assumed model for the dielectric loaded tape helix.

#### 4. NUMERICAL COMPUTATION OF THE DISPERSION CHARACTERISTIC

On using the asymptotic formulae for  $S_n$ ,  $S'_n$ ,  $T_n$  and  $T'_n$  [4], we observe from (17) that

$$|\sigma_n| \sim O(1/|n|) \text{ as } |n| \rightarrow \infty$$

Therefore, the rapidly converging infinite series for  $\alpha_{kq}$ ,  $k, q \in \mathbb{Z}$ , may be symmetrically truncated to a low order without incurring any appreciable error. When the accurate estimates for the matrix entries obtained in this fashion are used in the approximate dispersion equation resulting from a symmetric truncation of the infinite-order matrix  $\mathbf{A}$  to a matrix  $\hat{\mathbf{A}}$  of order  $(2N+1) \times (2N+1)$ , the corresponding dispersion characteristic is found to be almost insensitive to the truncation order  $N$  as long as  $N \geq 10$ .

The approximate dispersion equation for a truncation order  $N = 20$  and for the parameter values of  $\hat{w} = 1/2$ ,  $b/a = 2.24$ ,  $\epsilon_{\text{eff}} = 2.25$ , and  $\psi = 10^\circ$  is solved numerically for  $k_{0a}(\beta_{0a})$ ,  $\beta_{0a} \geq 0$ , and the resulting lowest order tape-helix dispersion curve is plotted in Fig. 2. It is worth emphasizing that the dispersion characteristic for a dielectric-loaded tape helix in the form shown in Fig. 2 has so far not been reported in the literature. Although there exists no forbidden region for the dielectric loaded tape helix, forbidden regions of an open tape helix for the same values of  $\hat{w}$  and  $\psi$  are also plotted in Fig. 2 for comparison

purposes. It is seen that the dispersion characteristic enters the first allowed region (slow wave region) of the anisotropically conducting model of open tape helix from the fast wave region. The dispersion curve first increases with increase in  $\beta_{0a}$  and then decreases as seen from Fig. 2. The characteristic reaches approximately zero at the meeting point of the forbidden region boundaries and increases as it enters the second allowed region of the open tape helix model. The peak value of the dispersion curve in the second ‘allowed region’ is slightly more than the peak value in the first ‘allowed’ region. The shape of the dispersion curve in the second ‘allowed’ region is then seen to repeat periodically in the subsequent ‘allowed’ regions also. The dominant-mode dispersion curve of a dielectric loaded sheath helix for the same values of  $\epsilon_{eff}$  and  $b/a$  is also plotted for comparison in Fig. 2. It is observed that the dielectric loaded sheath helix model is no longer an approximation to the dielectric loaded tape helix model.

In addition to the lowest order mode, whose dispersion curve is plotted in Fig. 2, a dielectric-loaded tape helix supports an infinite number of higher order modes. The dispersion curves for the modes of order from second to fifth are plotted in Fig. 3 together with that of the lowest order mode. The initial behaviour of the dispersion curves of modes higher than the second tend to be characteristically different from that of the first two modes for the parameter values of the helix assumed in the numerical computation. This “chaotic” behaviour may be attributed to the larger values of the “cut-off frequencies” of the

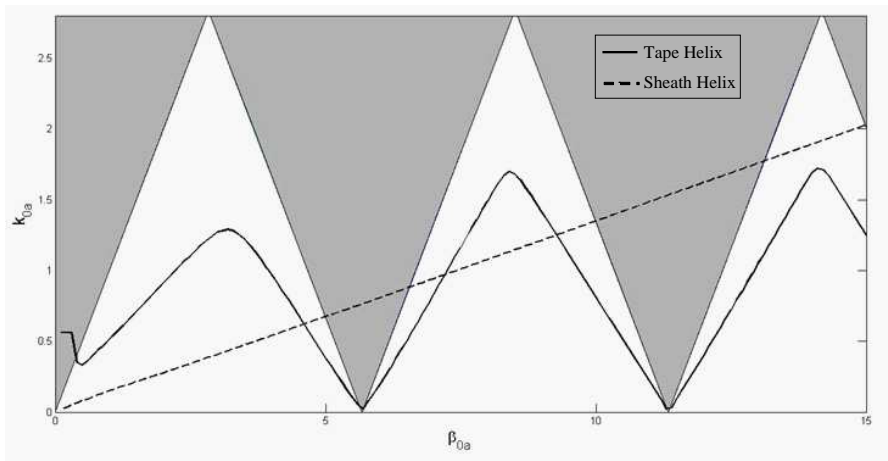


**Figure 2.** Dispersion characteristic of dielectric loaded tape helix for  $\hat{w} = 1/2$ ,  $b/a = 2.24$ ,  $\epsilon_{eff} = 2.25$  and  $\psi = 10^\circ$ .

higher order waveguide modes; the outer conductor may be considered as forming a circular cylindrical waveguide which is loaded by the anisotropically conducting tape helix and the partially filled dielectric layer. However, all these higher-order dispersion curves tend to merge eventually with the lowest-order dispersion curve along its negative-slope portion in the first ‘allowed’ region. Rest of the analysis in this paper will be making use of only the lowest-order mode dispersion characteristic.

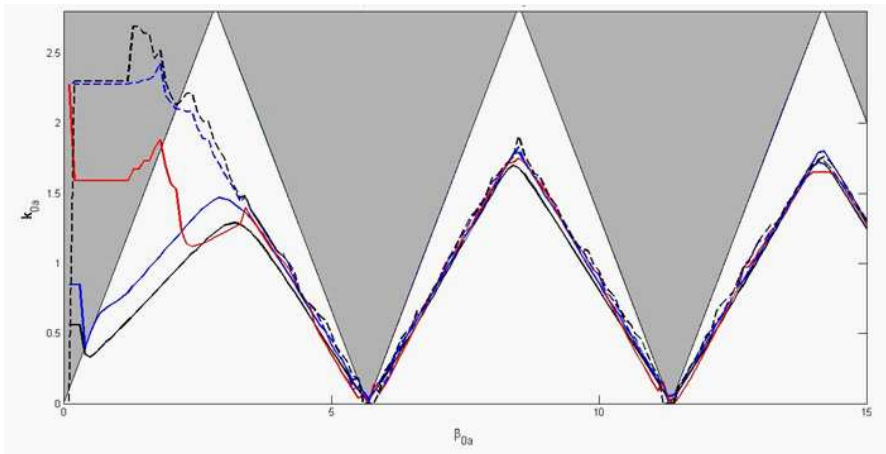


Figure 3. Dispersion characteristics for modes of first five orders.

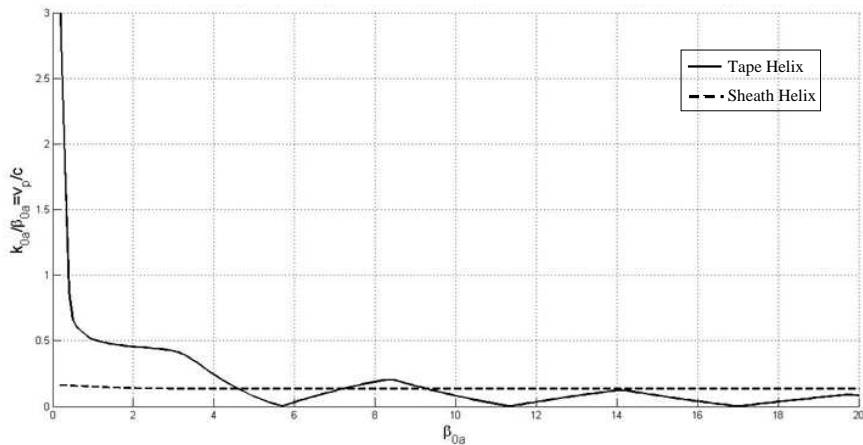
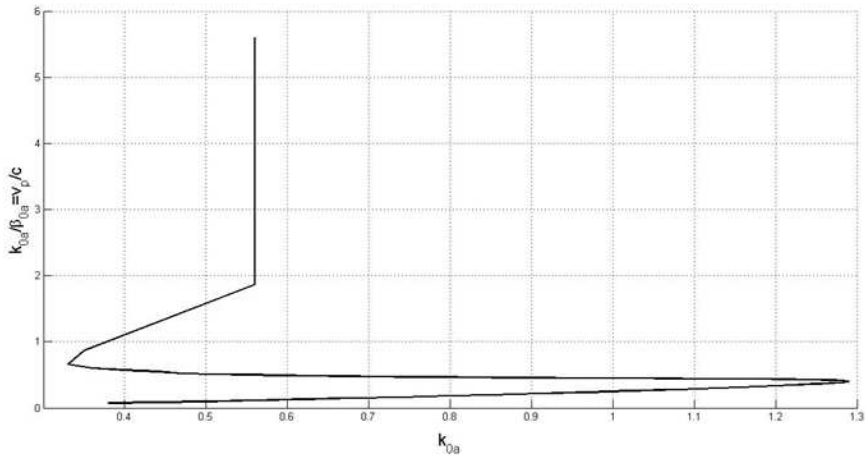


Figure 4. Plot of phase speed vs  $\beta_{0a}$ .

It is observed from the phase-speed plot of Fig. 4 that the phase speed  $v_p$  of the dielectric loaded sheath helix is approximately 13% of the speed of light. It is also seen from Fig. 4 that the phase speed of the dielectric loaded tape helix is more than two times that of the speed of light for very small values of  $\beta_{0a}$  ( $\beta_{0a} < 0.3$ ). As soon as the dispersion curve enters the first ‘allowed region’, the phase speed reduces to 50% of the speed of the light. Towards the end of the first ‘allowed region’ and thereafter, the phase speed varies from 1% and 20% of the speed of light. The only nearly constant phase speed region of the dielectric loaded tape helix useful for the purpose of effective interaction with an electron beam leading to traveling wave amplification corresponds to a value of  $\beta_{0a}$  lying between 1.5 and 3. It is to be noted that the phase speed of the dielectric loaded tape helix structure is 50% to that of the speed of light in the aforesaid region. For this reason, the relativistic effects (relativistic variation of electron mass with speed) have to be taken into account while analysing the beam-wave interaction in a TWT amplifier configuration.

The initial portion of the graph (of the multivalued function) showing the variation of the normalised phase speed  $v_p/c$  with respect to the normalised frequency  $k_{0a}$  for the dielectric loaded tape helix corresponding to  $0 < k_{0a} < 1.3$  is plotted in Fig. 5. It is observed from the plot that the normalised phase speed corresponding to the monotonically increasing portion of the dispersion curve (Fig. 2) in the first “allowed” region is nearly constant for  $k_{0a} \in (0.45, 1.28)$ .



**Figure 5.** Plot of phase speed vs  $k_{0a}$ .

For a helical radius  $a = 0.56896$  [18], it is found that the dielectric loaded tape helix may be operated in the frequency range of 4.2 GHz to 10.9 GHz, i.e., C-band and part of X-band of microwave frequencies.

### 5. NUMERICAL COMPUTATION OF THE TAPE CURRENT DISTRIBUTION

The distribution of current on the tape surface may be estimated in terms of the  $(2N + 1)$ -dimensional null-space vector  $\hat{\mathbf{J}}$  of the  $(2N + 1) \times (2N + 1)$  symmetrically truncated coefficient matrix  $\hat{\mathbf{A}}$  corresponding to any specified solution pair  $(\beta_{0a}, k_{0a}(\beta_{0a}))$  of the dispersion equation  $|\hat{\mathbf{A}}| = 0$ . Denoting the null-space vector of the corresponding singular matrix  $\hat{\mathbf{A}}$  by

$$\hat{\mathbf{J}} = \left[ \hat{J}_{-N}, \hat{J}_{-(N-1)}, \dots, \hat{J}_{-1}, \hat{J}_0, \hat{J}_1, \dots, \hat{J}_{N-1}, \hat{J}_N \right]^T \quad (23)$$

the surface current density for a truncation order  $N$  may be estimated using Fejer (Cesaro) means [19] as

$$\begin{aligned} \hat{J}_{\parallel}(z, \hat{\zeta}) &= e^{-j\beta_0 z} \hat{f}(\hat{\zeta}) \\ &= e^{-j\beta_0 z} \sum_{l \in \mathbb{Z}} 1_{[l-\hat{w}/2, l+\hat{w}/2]}(\hat{\zeta}) \sum_{n=-N}^N \left( 1 - \frac{|n|}{N+1} \right) \hat{J}_n e^{-j2\pi n \hat{\zeta}} \end{aligned} \quad (24)$$

The partial sum of Fourier series is estimated by Fejer means for a smoother approximation and faster convergence than is provided by the corresponding direct partial sums [20]. Since the surface-current density  $\hat{J}_{\parallel}(z, \hat{\zeta})$  is periodic in  $\hat{\zeta}$  with period 1, the restriction  $\hat{J}_{\parallel}^{(R)}(z, \hat{\zeta})$  of it to any one period, say to the interval  $[-1/2, 1/2]$ , gives a complete description:

$$\hat{J}_{\parallel}^{(R)}(z, \hat{\zeta}) = e^{-j\beta_0 z} 1_{[-1/2, 1/2]}(\hat{\zeta}) \sum_{n=-N}^N \left( 1 - \frac{|n|}{N+1} \right) \hat{J}_n e^{-j2\pi n \hat{\zeta}}$$

The magnitude  $|\hat{I}(\hat{\zeta})|$  and the phase  $\varphi(\hat{\zeta})$  of the normalized surface-current distribution

$$\begin{aligned} \hat{I}(\hat{\zeta}) &= \left| \hat{I}(\hat{\zeta}) \right| e^{j\varphi(\hat{\zeta})} \triangleq \frac{\hat{J}_{\parallel}^{(R)}(z, \hat{\zeta})}{\hat{J}_{\parallel}^{(R)}(z, 0)} \\ &= 1_{[-1/2, 1/2]}(\hat{\zeta}) \hat{f}(\hat{\zeta}) / \hat{f}(0) \\ &= 1_{[-1/2, 1/2]}(\hat{\zeta}) \frac{\sum_{n=-N}^N (1 - |n|/N + 1) \hat{J}_n e^{-j2\pi n \hat{\zeta}}}{\sum_{n=-N}^N (1 - |n|/N + 1) \hat{J}_n} \end{aligned} \quad (25)$$

computed for  $\beta_{0a} = 3$ ,  $\psi = 10^\circ$  and the values  $\frac{1}{2}$ ,  $\frac{5}{12}$  and  $\frac{1}{3}$  of the axial width-to-pitch ratio  $\hat{w}$  are plotted in Figs. 6–8 against  $\hat{\zeta} \in [-1/2, 1/2]$ .

It may be observed from the magnitude and the phase plots of the

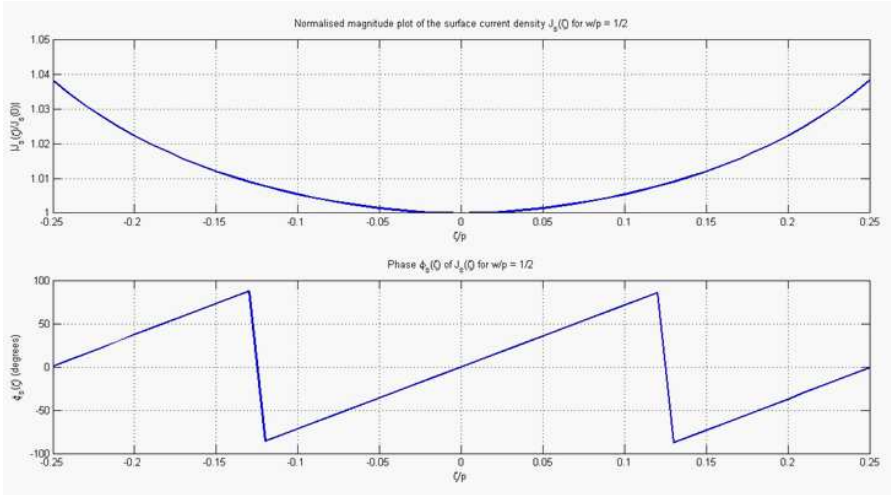


**Figure 6.** Surface current distribution of the anisotropically conducting dielectric-loaded tape-helix model for  $\hat{w} = \frac{1}{2}$ .

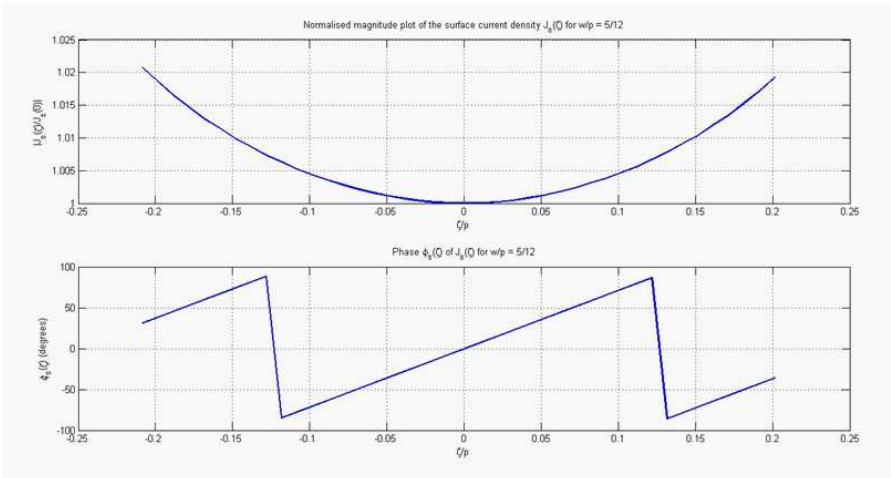


**Figure 7.** Surface current distribution of the anisotropically conducting dielectric-loaded tape-helix model for  $\hat{w} = \frac{5}{12}$ .

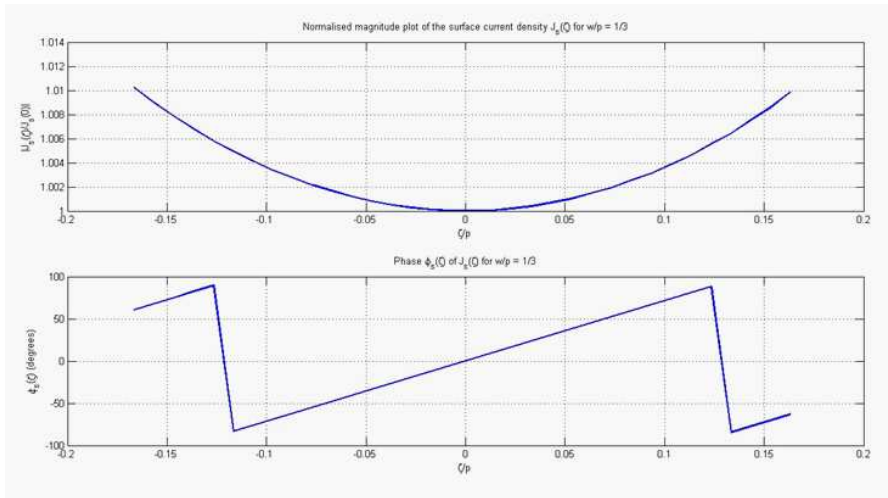


**Figure 8.** Surface current distribution of the anisotropically conducting dielectric-loaded tape-helix model for  $\hat{w} = \frac{1}{3}$ .

surface current distribution that

- (i) The magnitude distribution is even symmetric whereas the phase distribution is odd symmetric about the center line of the tape.
- (ii) The surface current density magnitude, which has a flat minimum along the center line of the tape, tends to grow superlinearly towards the tape edges, the edge value exhibiting a slight increase with the tape width; however the maximum deviation of the surface current density magnitude is less than 4% even for  $\hat{w} = 1/2$ .
- (iii) The phase of the surface current density, on the other hand, exhibits a periodic sawtooth variation across the tape width with two periods of the sawtooth waveform getting accommodated within the tape width when  $\hat{w} = 1/2$ ; as  $\hat{w}$  decreases, proportionately smaller portions of sawtooth waveform get accommodated within the width of the tape.

## 6. CONCLUSIONS

The main conclusions that may be drawn from the present study are the following: The dominant mode dispersion characteristic of the sheath helix is no longer a good approximation to that of the dielectric loaded tape helix. There are infinite number of modes supported

by a dielectric-loaded tape helix. The dispersion curves of higher order modes exhibit an initial 'chaotic' behaviour before eventually merging with the dispersion curve of the lowest-order mode. Only the lowest order mode dispersion curve is useful for the purpose of traveling-wave amplification. Effective electron beam-wave interaction for amplification purpose is only possible in the constant phase speed region of the first 'allowed region'. As this constant phase speed is nearly 50% of the speed of light, nonrelativistic operation of a helix traveling wave amplifier is no longer feasible; relativistic effects will have to be accounted for in the amplification process.

## REFERENCES

1. Kalyanasundaram, N. and G. N. Babu, "Dispersion of electromagnetic waves guided by an open tape helix I," *Progress In Electromagnetics Research B*, Vol. 16, 311–331, 2009.
2. Kalyanasundaram, N. and G. N. Babu, "Propagation of electromagnetic waves guided by an open tape helix," *IEEE International Vacuum Electronics Conference*, 185–186, Feb. 21–24, 2011.
3. Kalyanasundaram, N. and G. N. Babu, "Perfectly conducting tape-helix model for guided electromagnetic wave propagation," *IET Microwaves, Antennas & Propagation*, Vol. 6, No. 8, 899–907, Jun. 7, 2012.
4. Sensiper, S., "Electromagnetic wave propagation on helical conductors," Sc.D. Thesis, Massachusetts Institute of Technology, Cambridge, Mar. 1951.
5. Chodorov, M. and E. L. Chu, "Cross-wound twin helices for traveling-wave tubes," *J. Appl. Phys.*, Vol. 26, No. 1, 33–43, 1955.
6. Watkins, D. A., *Topics in Electromagnetic Theory*, John Wiley & Sons, New York, 1958.
7. Zhang, K. A. and D. Li, *Electromagnetic Theory for Microwaves and Optoelectronics*, 2nd Edition, Springer-Verlag, Berlin-Heidelberg, 2008.
8. Basu, B. N., *Electromagnetic Theory and Applications in Beam wave Electronics*, World Scientific, Singapore, 1996.
9. Jain, P. K. and B. N. Basu, "The inhomogeneous loading effects of practical dielectric supports for the helical slow-wave structure of a TWT," *IEEE Transactions on Electron Devices*, Vol. 34, No. 12, 2643–2648, Dec. 1987.
10. Tien, P. K., "Traveling-wave tube helix impedance," *Proceedings of the IEEE*, Vol. 41, No. 11, 1617–1623, Nov. 1953.

11. McMurtry, J. B., "Fundamental interaction impedance of a helix surrounded by a dielectric and a metal shield," *IEEE Transactions on Electron Devices*, Vol. 9, No. 2, 210–216, 1962.
12. Uhm, H. S., "Electromagnetic-wave propagation in a conducting waveguide loaded with a tape helix," *IEEE Transactions on Microwave Theory and Techniques*, Vol. 31, No. 9, 704–710, Sep. 1983.
13. D'Agostino, S., F. Emma, and C. Paoloni, "Accurate analysis of helix slow-wave structures," *IEEE Transactions on Electron Devices*, Vol. 45, No. 7, 1605–1613, 1998.
14. Tsutaki, K., Y. Yuasa, and Y. Morizumi, "Numerical analysis and design for high-performance helix traveling wave tubes," *IEEE Transactions on Electron Devices*, Vol. 32, No. 9, 1842–1849, 1985.
15. Kosmahl, H. G. and G. M. Branch, Jr., "Generalized representation of electric fields in interaction gaps of klystrons and traveling-wave tubes," *IEEE Transactions on Electron Devices*, Vol. 20, No. 7, 621–629, Jul. 1973.
16. Chen, Q., Z. Wang, and H. Wu, "The dispersion characteristics of vane loaded tape helix slow wave structure," *International Conference on Microwave and Millimeter Wave Technology Proceedings*, Beijing Vacuum Electronics Research Institute, Beijing, 1998.
17. Chernin, D., T. M. Antonsen, Jr., and B. Levush, "Exact treatment of the dispersion and beam interaction impedance of a thin tape helix surrounded by a radially stratified dielectric," *IEEE Transactions on Electron Devices*, Vol. 46, No. 7, 1472–1483, Jul. 1999.
18. Gilmour, A. S., *Klystrons, Traveling Wave Tubes, Magnetrons, Cross-Field Amplifiers, and Gyrotrons*, Artech House, 2011.
19. Katzenelson, Y., *An Introduction to Harmonic Analysis*, 3rd Edition, Cambridge University Press, 2004.
20. Davidson, K. R. and A. P. Dosig, *Real Analysis with Real Applications*, Prentice-Hall, 2002.